Proceedings, 6th African Rift Geothermal Conference
Addis Ababa, Ethiopia, 2nd – 4th November 2016

CHEMICAL AND ISOTOPIC CHARACTERISTICS OF THE FUMAROLES OF ALUTO VOLCANO, ETHIOPIA

C. Pasqua[1], W. Melesse[2], A. Teclu[2], L. Marini[1]

[1]ELC-Electroconsult, Via Marostica, 1, 20146 Milano, Italy
[2] Geological Survey of Ethiopia, P.O. Box 2032, Addis Ababa, Ethiopia

e-mail: claudio.pasqua@elc-electroconsult.com

ABSTRACT

The fumarolic manifestations of Gebiba and Finkilo discharge gas mixtures practically free of air and Air-Saturated Water (ASW) with high CO_2, relatively high CH_4, and low H_2S, H_2, CO, He, Ar and N_2, indicating that the deep CO_2-rich gases do not interact with shallow aquifer(s) in these sites. Gas geothermometers indicate initial (reservoir) temperatures of 295-330°C for the Finkilo fumaroles and 200-250°C for the Gebiba fumaroles. Gas geothermometers and stable water isotopes indicate occurrence of vapor/liquid separation close to 100°C at Gebiba. Due to the possible occurrence of steam condensation, gas geothermometers do not constrain the vapor/liquid separation temperature of Finkilo fumarolic effluents. Stable water isotopes indicate vapor/liquid separation temperatures in the order of 155-170°C for the two best samples from Finkilo fumaroles.
All the fumarolic manifestations other than Finkilo and Gebiba release gas mixtures dominated by ASW with low (or relatively low) CO_2, low CH_4, and undetectable H_2S, H_2, He and CO. The abundance of ASW in these fumarolic gases suggests that the deep CO_2-rich gases interact with a shallow aquifer which is evidently in contact with the atmosphere. These fumarolic manifestations containing significant proportions of ASW and unsuitable for the application of gas geothermometers have the following vapor/liquid separation temperatures, based on stable water isotopes: 150-180°C for Kure, 150°C for Oitu, 135-95°C Bobessa, 100°C for Auto and ~95°C Hulo.
Summing up, the highest vapor/liquid separation temperatures are found: (a) along the NNE-trending Jawe Fault, passing through Finkilo and possibly Oitu, and (b) along the NNE-trending tectonic structure passing through Kure and possibly Bobessa. Consequently, these tectonic structures locally act as main upflow zones of the Aluto-Langano geothermal system. In contrast, the peripheral fumarolic manifestations of Gebiba, Auto and Hulo have low vapor/liquid separation temperatures, indicating that they may represent lateral discharge zones of the Aluto geothermal system.

1. INTRODUCTION

Weak fumaroles and steaming grounds are widely distributed within the Aluto volcano, in association with faults and fractures. These fumarolic manifestations were studied in the past by Glover (1976), Craig and Lupton (1977) and Darling (1998). During these previous works some fumaroles and steaming grounds were not sampled and some parameters were not determined, such Ar, He, CO and, in some instances, the stable isotopes of H_2O. In addition, the precise location of sampling points is unknown, since geographical coordinates are not given in previous studies, where only locality names and poor-quality sketch maps are given. Therefore, the fumaroles and steaming grounds of Aluto were surveyed again during this work, carried out in the framework of the NDF-ICEIDA Geothermal exploration project.

2. SAMPLING AND LABORATORY ANALYSIS

Nineteen gas samples were collected during the geochemical survey carried out in October 2015. The location of the sampled fumaroles and steaming grounds is shown in the map of Figure 1, whereas

geographical coordinates are given together with the results of chemical analyses in Table 1 and together with the results of isotopic analyses in Table 2.

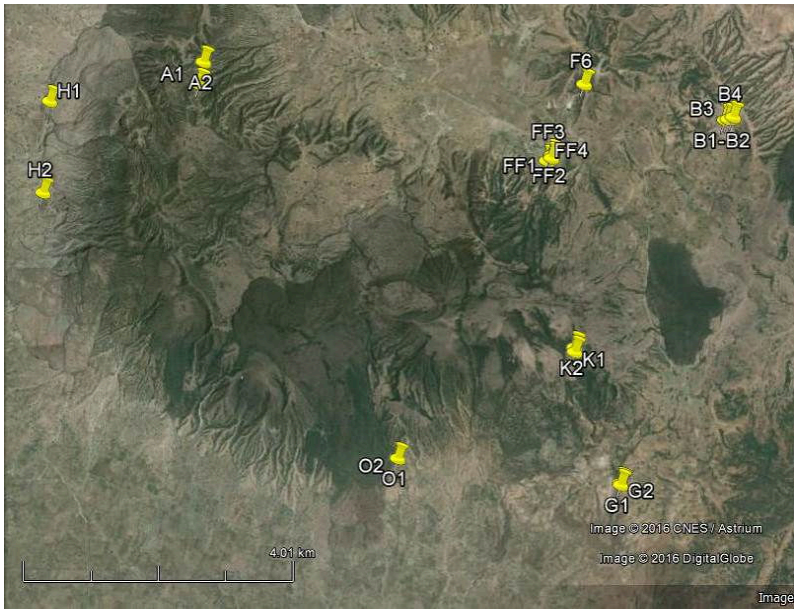

Figure 1: Location map of the Aluto fumaroles and steaming grounds sampled during this work.

Apart from the fumaroles of Gebiba, all the other manifestations are characterized by low-pressure gas emissions (steaming grounds). Odour of rotten eggs is either lacking or scarcely perceptible, indicating nil to low contents of hydrogen sulfide. Red soils are present in these manifestations, suggesting the occurrence of relatively mild alteration, similar to the weathering processes leading to lateritic soils, probably due to absence or scarcity of H_2S in Aluto gas discharges.

At each sampling point we obtained samples of total fluids in Giggenbach's bottles as well as samples of dry gases and steam condensates by using a sampling line comprising a glass condenser-separator cooled by circulating cold water. However, it was not possible to collect steam condensates from the steaming grounds close to well LA-6 (sample F6) and Adonsha (samples A1 and A2) owing to the very low H_2O concentration. In addition, only the bottle for total fluids analysis was obtained for sample B2 which is the duplicate of sample B1.

Incondensable inorganic gases (N_2, O_2, H_2, He and Ar) collected in the Giggenbach's bottles were analysed using a Shimadzu 15A GC equipped with a 10 m long 5Å molecular sieve column and a TCD. To split Ar from O_2, temperature was lowered to 0°C using a cryogenic liquid CO_2 cooling loop Shimadzu CRG-15. Since CO was undetectable in dry gas samples, it was determined in the gas phase collected in the Giggenbach's bottles, after conversion to CH_4 at 400°C, by using the same GC equipped with a FID and employing a MS 5 Å 1/8' × 50' column and H_2 as carrier gas. Carbon dioxide was measured on the alkaline solution by titration with a 0.5 N HCl solution using an automatic titrator Metrohm Basic Titrino. Hydrogen sulfide was also measured on the alkaline solution through peroxide oxidation of sulfide to sulfate, which was then determined by ion-chromatography using a Metrohm IC 761. Water was obtained by difference between the amount of sample collected and the amounts of all other gas constituents. All obtained chemical data have analytical uncertainties ≤5% for the main gas components and ≤10% for minor and trace gas species. The concentrations of gas constituents are reported on a dry gas basis and water concentration is given separately, owing to the impossibility to determine H_2O concentration for several samples collected in Giggenbach's flask and considering the uncertainty on this parameter. The H_2O concentration called H_2O lab in Table 1 was obtained from the analysis of Giggenbach's flasks. The H_2O content named H_2O field in Table 1 was evaluated on the basis of the volume of dry gas pumped through the sampling line and the related amount of steam condensate. The two series of data agree at high H_2O contents (Gebiba, Auto and Hulo, which have outlet temperature close to the boiling point of pure water) whereas they deviate considerably for H_2O-field lower than 875-900 mmol/mol.

Table 1: Results of the chemical analyses of the gas samples collected from the Aluto fumarolic manifestations during this work. UTM coordinates are consistent with the WGS84 geodetic datum. H is altitude, T is outlet temperature. Concentrations of all gas species, except water, are on a dry basis. Hyphen means below detection limit.

Code	UTM-E	UTM-N	T	CO_2	H_2S	N_2	CH_4	Ar	O_2	H_2	He	CO	H_2O lab	H_2O field
	m	m	°C	mmol/mol on a dry basis									mmol/mol in total	
B1	479978	861048	90.7	395	-	413	0.039	9.5	182	-	-	-	-	927
B2	479978	861048	90.7	432	-	406	0.064	9.4	153	-	-	-	-	927
B3	480027	861059	90.9	296	-	503	0.13	11	190	-	-	-	-	898
B4	480098	861089	89.2	385	-	439	0.10	11	165	-	-	-	-	835
F6	477936	861561	81.9	335	-	474	0.085	12	179	-	-	-	-	(543)
FF1	477459	860515	90.4	971	6.6	21	0.39	0.38	0.15	0.26	0.011	0.0007	945	825
FF2	477461	860554	90.0	959	4.9	5.6	19	0.12	0.16	11	0.0046	0.0009	905	860
FF3	477458	860560	89.9	950	5.9	7.5	23	0.14	0.24	13	0.0061	0.0005	931	807
FF4	477390	860474	91.2	988	2.9	4.2	3.5	0.080	0.09	0.79	0.0029	0.0011	923	908
K1	477801	857760	90.0	12.0	-	707	0.011	17	264	-	-	-	-	821
K2	477800	857822	90.2	258	-	524	0.013	12	206	-	-	-	-	854
G1	478454	855836	92.8	993	0.9	3.6	2.5	0.060	0.070	0.11	0.0021	0.0004	990	985
G2	478449	855862	93.5	994	0.6	3.3	1.4	0.050	0.060	0.21	0.0023	0.0005	991	990
A1	472403	861540	77.9	11.0	-	727	0.016	18	244	-	-	-	-	(392)
A2	472451	861862	82.1	5.90	-	787	0.037	19	188	-	-	-	-	(551)
H1	470040	861363	93.5	492	-	385	0.21	9.2	113	-	-	-	962	962
H2	469926	860047	93.1	449	-	415	0.18	10	126	-	-	-	948	955
O1	475176	856215	93.2	100	-	645	0.023	16	239	-	-	-	-	965
O2	475169	856220	93.1	140	-	617	0.031	15	228	-	-	-	-	967

The steam condensate samples were used to determine the δ^2H values (reproducibility ±1‰) and $\delta^{18}O$ values (reproducibility ±0.1‰) of water by TC-IRMS and DI-IRMS, respectively. The $\delta^{13}C$ value of CO_2 was determined on the dry gas sample using a Delta S (Finnigan) mass spectrometer, after standard extraction and purification procedures of the dry gas mixtures. The analytical uncertainties and the reproducibility are ±0.05‰ and ±0.1‰, respectively.

3. THE CHEMISTRY OF THE ALUTO FUMAROLIC MANIFESTATIONS

Aluto fumarolic manifestations are dominated by water vapor, with H_2O concentration of 807 to 990 mmol/mol in total fluids, although H_2O concentration is unknown for the steaming grounds of A1, A2, F6. The triangular plots of CO_2-N_2-O_2 (Figure 2a) and CO_2-N_2-Ar (Figure 2b) show that: (i) the fumarolic manifestations of Gebiba and Finkilo discharge gas mixtures practically free of air and air-saturated water (ASW), with high CO_2 contents; (ii) all the other fumarolic manifestations release gas mixtures dominated by ASW with a subordinate proportion of the CO_2-rich component; based on Ar, the fraction of ASW is 0.98-0.99 at Adonsha, 0.87-0.91 at Oitu, 0.76-0.98 at Kore, 0.68 in the vent close to well LA-6, 0.58-0.72 at Bobessa, 0.58 at Hulo, and 0.55 at Auto.

It must be underscored that ASW (not air) is present in the gas mixtures discharged at Adonsha, Oitu, Kore, vent close to well LA-6, Bobessa, Hulo, and Auto as clearly shown by the N_2/Ar ratio (see Figure 2b). The N_2/O_2 ratio (see Figure 2a) is misleading due to occurrence of redox reactions with partial consumption of O_2 and consequent increase in the N_2/O_2 ratio.

The occurrence of these redox reactions is testified by the virtual absence of the fast-reacting reduced gases (i.e., H_2S, H_2, and CO) in the gas mixtures discharged at Adonsha, Oitu, Kore, vent close to well LA-6, Bobessa, Hulo, and Auto. The involvement of ASW (not air) in the fumarolic gases discharged at Adonsha, Oitu, Kore, close to well LA-6, Bobessa, Hulo, and Auto suggests that in these sites the

deep CO_2-rich gases interact with a shallow aquifer which is evidently in contact with the atmosphere. In contrast, the virtual absence of ASW in the fumarolic gases released at Gebiba and Finkilo indicates that the deep CO_2-rich gases do not interact with a shallow aquifer in these sites.

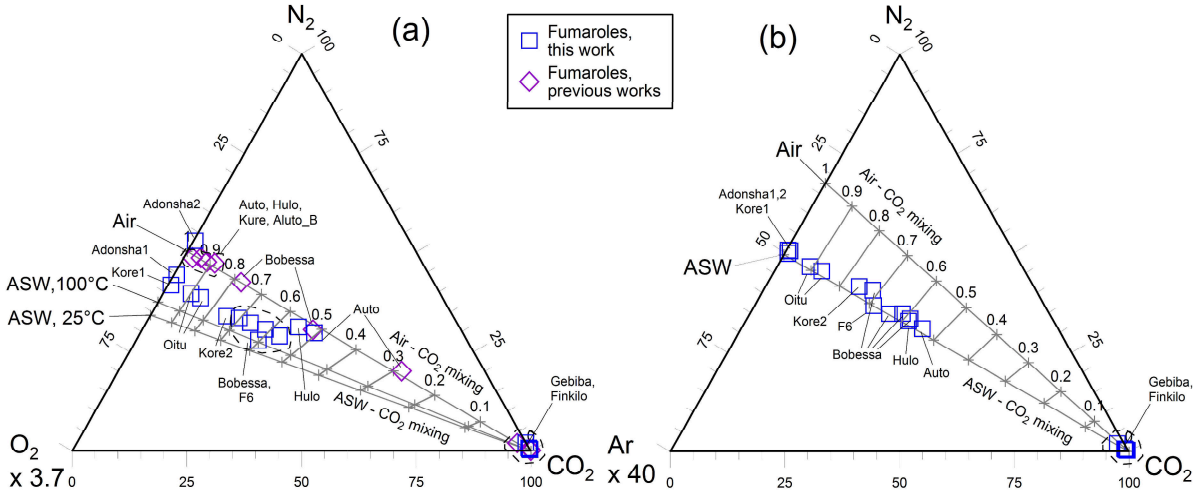

Figure 2: Triangular diagrams of (a) CO_2-N_2-O_2 and (b) CO_2-N_2-Ar for the fumarolic manifestations sampled during this work and in previous studies. The air-CO_2 and the ASW-CO_2 mixing lines are also shown (numbers indicate the fraction of air or ASW in the gas mixtures).

Table 2: Results of the isotopic analyses of CO_2 and steam condensates collected from the Aluto fumarolic manifestations during this work. UTM coordinates are consistent with the WGS84 geodetic datum. H is altitude, T is outlet temperature, n.a. means not analysed.

Code	Date	UTM-E	UTM-N	H	T	δ^2H-H_2O	δ^{18}O-H_2O	δ^{13}C-CO_2
		m	m	m asl	°C	‰ vs. V-SMOW		‰ vs. V-PDB
B1	23/10/2015	479978	861048	1991	90.7	-26.3	-6.12	-4.06
B2	23/10/2015	479978	861048	1991	90.7	n.a.	n.a.	n.a.
B3	23/10/2015	480027	861059	2000	90.9	-36.3	-7.20	-4.04
B4	23/10/2015	480098	861089	2027	89.2	-35.8	-7.35	-4.07
F6	23/10/2015	477936	861561	2021	81.9	n.a.	n.a.	-3.69
FF1	24/10/2015	477459	860515	1952	90.4	-42.5	-8.93	-3.90
FF2	24/10/2015	477461	860554	1942	90.0	-28.9	-6.90	-3.89
FF3	24/10/2015	477458	860560	1930	89.9	-34.2	-7.87	-3.04
FF4	24/10/2015	477390	860474	1965	91.2	-26.7	-6.07	-3.92
K1	25/10/2015	477801	857760	2055	90.0	-28.5	-7.11	-4.59
K2	25/10/2015	477800	857822	2055	90.2	-38.8	-8.56	-4.91
G1	25/10/2015	478454	855836	1818	92.8	-38.1	-7.41	-3.87
G2	25/10/2015	478449	855862	1818	93.5	-35.4	-7.03	-3.61
A1	26/10/2015	472403	861540	2141	77.9	n.a.	n.a.	-5.25
A2	26/10/2015	472451	861862	2103	82.1	n.a.	n.a.	-5.00
H1	26/10/2015	470040	861363	1734	93.5	-43.0	-8.46	-5.66
H2	26/10/2015	469926	860047	1749	93.1	-37.2	-7.06	-5.25
O1	27/10/2015	475176	856215	1807	93.2	-29.8	-7.00	-3.23
O2	27/10/2015	475169	856220	1815	93.1	-30.7	-7.21	-4.65

Only the samples of Gebiba and Finkilo are shown in the N_2-Ar-He triangular plot (Figure 3) since He is undetectable in all the other gas mixtures. Data from previous studies are not shown since He was

not measured. The low Ar/He and N_2/He ratios of Gebiba and Finkilo gases are probably due to addition of helium deriving from the mantle source to the gases supplied from the meteoric source. The involvement of mantle gases rather than crustal gases is suggested by the location of Aluto within the area affected by the so-called Ethiopian mantle plume (Craig and Lupton, 1977).

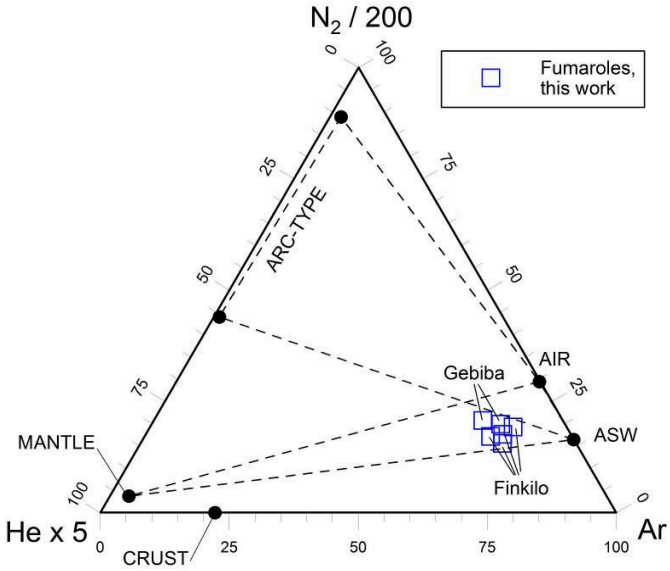

Figure 3: Triangular diagram of N_2-Ar-He (after Giggenbach, 1991) for the Aluto fumarolic manifestations sampled during this work. The endmember compositions of crustal, mantle, and arc-type gases are also shown.

4. GAS EQUILIBRIA

Gas equilibria are investigated by means of binary plots which are based on the approach of Chiodini and Marini (1998) and display the chemical composition of the vapors separated in a single-step, at temperature Ts, from a boiling liquid of initial (reservoir) temperature To. Where needed, redox conditions are fixed by the FeO-$FeO_{1.5}$ hydrothermal buffer of Giggenbach (1987) or Fayalite-Hematite-Quartz (FHQ) buffer. In most geothermal systems, this redox buffer fixes the logarithm of the H_2/H_2O fugacity ratio at -2.82 ± 0.02, independent of temperature (Giggenbach, 1987), although different redox buffers, rather than the FHQ only, may be present in distinct geothermal systems or even in different parts of the same system (Chiodini and Marini, 1998 and references therein).
Gas geothermometers can be applied to the fumarolic fluids of Finkilo and Gebiba only, whereas all the other fumarolic manifestations, containing significant proportions of ASW, are unsuitable for the application of gas geothermometers

4.1. The H_2-based geothermometers

Owing to the totally unreactive nature of Ar and the nearly similar behaviour of N_2, the geothermometric functions involving the H_2/N_2 ratio and the H_2/Ar ratio (Arnórsson, 1987; Giggenbach, 1991) are essentially H_2-geothermometers and are expected to indicate the same equilibrium temperature of the H_2/H_2O ratio unless interfering processes (air addition, irreversible loss of Ar or N_2, steam condensation and H_2O addition) take place (Figure 4).
The fumarolic gases sampled at Gebiba indicate low separation temperatures (T_S close to 100°C) from boiling liquids of initial (reservoir) temperature T_O in the 220-240°C based on the H_2/H_2O ratio and 190-220°C range based on the H_2/N_2. Low T_S values and similar T_O values, 200-225°C, and are also indicated by the H_2/Ar ratio.
The fumarolic gases collected at Finkilo during this work show considerable differences in their H_2/Ar, H_2/N_2 and H_2/H_2O ratios. Samples FF1 and FF4 are probably affected by addition of atmospheric air and either water addition or vapor separation at relatively low temperatures. Accepting that samples FF2 and FF3 are not influenced by interfering processes (although the

occurrence of steam condensation cannot be totally excluded), they are either high-temperature equilibrium vapors or vapors separated from boiling liquids at high temperatures T_S, close to the initial (reservoir) temperature T_O of 295-300°C (based on the H_2/Ar ratio) or 325-330°C (based on the H_2/N_2 ratio).

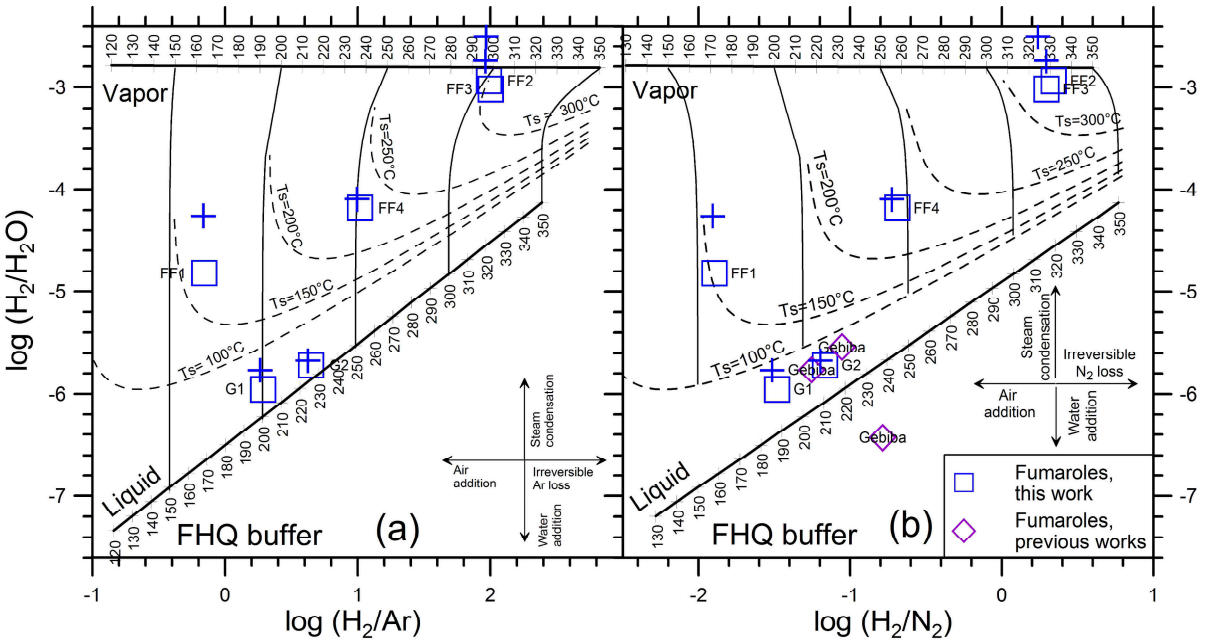

Figure 4: Diagrams of (a) log(H_2/Ar) vs. log(H_2/H_2O) and (b) log(H_2/N_2) vs. log(H_2/H_2O) for the Aluto fumarolic manifestations. The chemical compositions computed from both H_2O-lab data (blue squares) and H_2O-field data (blue crosses) are shown. The diagrams also show the theoretical compositions expected for gas equilibration in a saturated pure vapor phase (vapor line) and in a saturated pure liquid phase (liquid line), under redox conditions controlled by the FHQ redox buffer, as well as the effects of steam separation at temperature T_S on liquids initially equilibrated at temperature $T_O > T_S$ and possible interfering processes.

4.2. The CO-CO_2 and CH_4-CO_2 geothermometers

In the diagram of log(CH_4/CO_2) vs. log(H_2/H_2O) (Figure 5a) the samples FF2 and FF3 from Finkilo (the most representative ones from this fumarolic manifestations, see above) are positioned close to the vapor line at high reservoir temperatures (T_O of 300-305°C) whereas the samples from Gebiba are situated below the liquid line. The gas mixtures of Gebiba exhibit a marked disequilibrium between the H_2-H_2O subsystem and the CH_4-CO_2 subsystem, which might be due to the slow kinetics of CH_4-CO_2 re-equilibration upon cooling, especially at relatively low temperatures (Giggenbach, 1997). Accepting this explanation, the high T_O values indicated by the CH_4/CO_2 ratio (≥ 340°C) might be present at a large distance from the Gebiba gas manifestation. Alternatively, these high T_O values might be inexistent.

In the diagram of log(CO/CO_2) vs. log(H_2/H_2O) (Figure 5b), the gas mixtures of Gebiba indicate occurrence of vapor separation at low temperatures (close to 100°C) from boiling liquids of initial (reservoir) temperature T_O in the 175-180°C range. The samples FF2 and FF3 from Finkilo (the ones less affected by interfering processes among those collected from this fumarolic manifestations, see above) are found close to the vapor line also in this plot, but indicate low reservoir temperatures (T_O of 100-120°C), in striking contrast with all other gas constituents of geothermometric interest.

The low reservoir temperatures indicated by the CO-CO_2 geothermometer probably reflect underestimation of the CO content of the sampled gas mixtures due to partial conversion of CO to sodium formate through reaction with excess NaOH present in the Giggenbach's bottles (Giggenbach and Matsuo, 1991). Hence, it is advisable to neglect the apparent equilibrium temperatures indicated by the CO-CO_2 geothermometer.

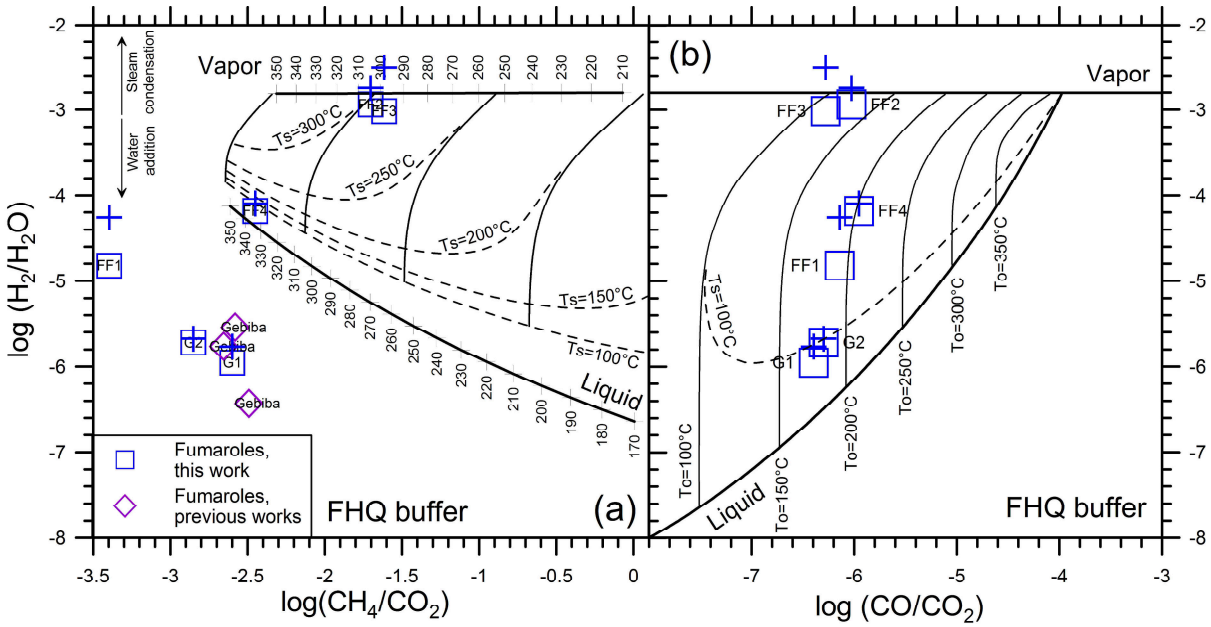

Figure 5: Diagrams of (a) $\log(CH_4/CO_2)$ vs. $\log(H_2/H_2O)$ and (b) $\log(CO/CO_2)$ vs. $\log(H_2/H_2O)$ for the Aluto fumarolic manifestations. The chemical compositions computed from both H_2O-lab data (blue squares) and H_2O-field data (blue crosses) are shown. The diagrams also show the theoretical compositions expected for gas equilibration in a saturated pure vapor phase (vapor line) and in a saturated pure liquid phase (liquid line), under redox conditions controlled by the FHQ redox buffer, as well as the effects of steam separation at temperature T_S on liquids initially equilibrated at temperature $T_O > T_S$.

4.3. Synthesis of gas geothermometric results

Finkilo - Assuming that samples FF2 and FF3 are not influenced by interfering processes, they appear to be either high-temperature equilibrium vapors or vapors separated from boiling liquids at high temperatures, T_S, close to the initial (reservoir) temperature, T_O, in all the considered geothermometric plots. To is 295-300°C based on the H_2/Ar ratio, 300-305°C based on the CH_4/CO_2 ratio, and 325-330°C based on the H_2/N_2 ratio. If so, these fumarolic manifestations would be situated along a major upflow zone of the Aluto geothermal system. Accepting instead that samples FF2 and FF3 are affected by steam condensation, the separation temperatures indicated by gas geothermometers would be overestimated whereas the initial (reservoir) temperature would be in the same range.
Gebiba – Gas mixtures from this site are consistent with occurrence of vapor separation at low temperatures (close to 100°C). The different geothermometers provide different indications for the initial (reservoir) temperature T_O of the liquid phase, namely 190-220°C (H_2/N_2), 200-225°C (H_2/Ar), 220-240°C (H_2/H_2O) and ≥ 340°C (CH_4/CO_2). These different indications might reflect the different kinetics of re-equilibration of each geothermometric subsystem. However, the high T_O values indicated by the CH_4/CO_2 ratio might be inexistent. If so, the initial (reservoir) temperature T_O of the liquid phase would be in the range 200-250°C approximately.

5. THE δ^2H AND $\delta^{18}O$ VALUES OF FUMAROLIC STEAM CONDENSATES

The δ^2H and $\delta^{18}O$ values of the fumarolic steam condensates from the study area obtained during this work (data in Table 2) and from previous studies (Craig and Lupton, 1977 and Darling and Talbot, 1991) are reported in the correlation plot of Figure 6, together with the isotope values of the reservoir liquids of the geothermal wells LA-3, LA-4, LA-6, and LA-8 (Darling et al., 1996; Teklemariam and Beyene, 2002). Since the geothermal reservoir liquids distribute in two clusters, one comprising wells LA-3 and LA-8, the other including wells LA-6 and LA-4, the average δ^2H and $\delta^{18}O$ values of the reservoir liquids of wells LA-3 and LA-8 (δ^2H = -9.55 ‰; $\delta^{18}O$ = -2.42 ‰) and of the reservoir liquids of wells LA-6 and LA-4 (δ^2H = -10.17 ‰; $\delta^{18}O$ = -1.41 ‰) are also shown. These average

δ^2H and $\delta^{18}O$ values were used to predict the theoretical effects of both (i) single-step steam separation (boiling), adopting the approach of Giggenbach and Stewart (1982) and (ii) Rayleigh condensation at 95°C (e.g., Faure, 1986). Liquid-vapor fractionation factors of O and H isotopes were computed using the relations of Horita and Wesolowski (1994) for pure water.

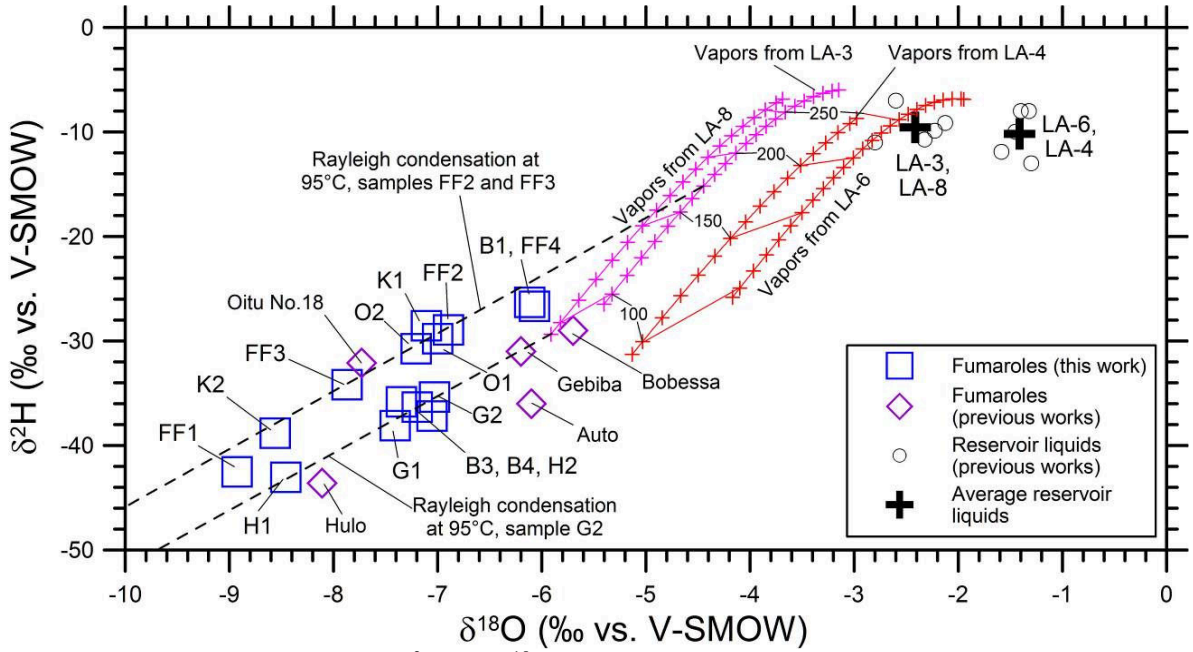

Figure 6: Correlation diagram of δ^2H vs. $\delta^{18}O$ values for the fumarolic steam condensates from the study area obtained during this work and from previous studies. The isotope values of the geothermal wells LA-3, LA-4, LA-6, and LA-8 are also plotted. Also shown are the theoretical isotope composition of the vapors separated at decreasing temperature (at steps of 10°C, until 100°C and at 95°C) through single-step boiling of the reservoir liquids of wells LA-3 (T_O = 307°C), LA-8 (T_O = 266°C), LA-6 (T_O = 323°C), and LA-4 (T_O = 246°C). The theoretical effects of Rayleigh condensation at 95°C of sample B1 are also displayed.

The δ^2H and $\delta^{18}O$ values of the vapors separated in a single step at decreasing temperatures T_S (at intervals of 10°C, until 100°C and at 95°C) from the reservoir liquids of wells LA-3 (T_O = 307°C), LA-8 (T_O = 266°C), LA-6 (T_O = 323°C), and LA-4 (T_O = 246°C) were computed adopting the average δ^2H and $\delta^{18}O$ values indicated above. Results are represented in Figure 6 by the red lines and crosses for the vapors from wells LA-6 and LA-4 and by the purple lines and crosses for the vapors from wells LA-3 and LA-8.

The theoretical effects of Rayleigh condensation at 95°C for sample G2 from Gebiba and for samples FF2 and FF3 from Finkilo are indicated by the two black dashed lines in Figure 6. Condensation lines with the same slope (which is fixed by the assumed condensation temperature of 95°C) can be drawn for all the other steam condensate samples.

The condensation line of sample G2 intersects the "line of vapors from LA-8" at a separation temperature T_S of 95°C. A similar T_S is indicated by the intersection of the condensation line of sample G1 (not shown) and the "line of vapors from LA-8". These low T_S values pointed out by the stable isotopes of water for the Gebiba fumaroles are in excellent agreement with the T_S values close to 100°C which are suggested by gas geothermometry (see above).

The condensation lines of samples FF2 and FF3 are superimposed in Figure 6. They intersect the "line of vapors from LA-8" at a T_S of 155°C and the "line of vapors from LA-3" at a T_S of 170°C whereas they do not intersect the LA-4 and LA-6 boiling lines. These T_S values are lower than the high T_S values, close to the initial (reservoir) temperature of 295-330°C, which are suggested by gas geothermometry (see above) assuming that samples FF2 and FF3 are not influenced by steam condensation (and other interfering processes). Accepting instead that samples FF2 and FF3 are affected by steam condensation, the T_S values suggested by gas geothermometers would be

overestimated. All in all, it is reasonable to conclude that vapor/liquid separation temperatures are probably in the order of 155-170°C for the Finkilo fumaroles, also considering that the stable isotopes of water indicate T_S values of 125°C for samples FF1 and FF4.
Let us now consider the steam condensates of the other fumarolic manifestations, containing significant proportions of ASW and unsuitable for the application of gas geothermometers. The intersection of the "line of vapors from LA-8" (which is taken as reference based on previous discussion) and the condensation line of each of these fumarolic manifestations indicates the following vapor/liquid separation temperatures: (i) 180°C for sample K1 and 150°C for sample K2, both from Kure; (ii) 150°C for samples O1 and O2, both from Oitu; (iii) 135°C for sample B1, 105°C for sample B4, and 95°C for sample B3, all from Bobessa; (iv) 100°C for sample H1 from Auto; (v) about 95°C for sample H2 from Hulo.
The map of Figure 7 suggests that the highest vapor/liquid separation temperatures are found: (a) along the NNE-trending Jawe Fault, passing through Finkilo and possibly Oitu, and (b) along the NNE-trending tectonic structure passing through Kure and possibly Bobessa (note that separation temperatures are highly variable of Bobessa). In contrast, the peripheral fumarolic manifestations of Gebiba, Auto and Hulo have low vapor/liquid separation temperatures, indicating that they may represent lateral discharge zones of the Aluto geothermal system.

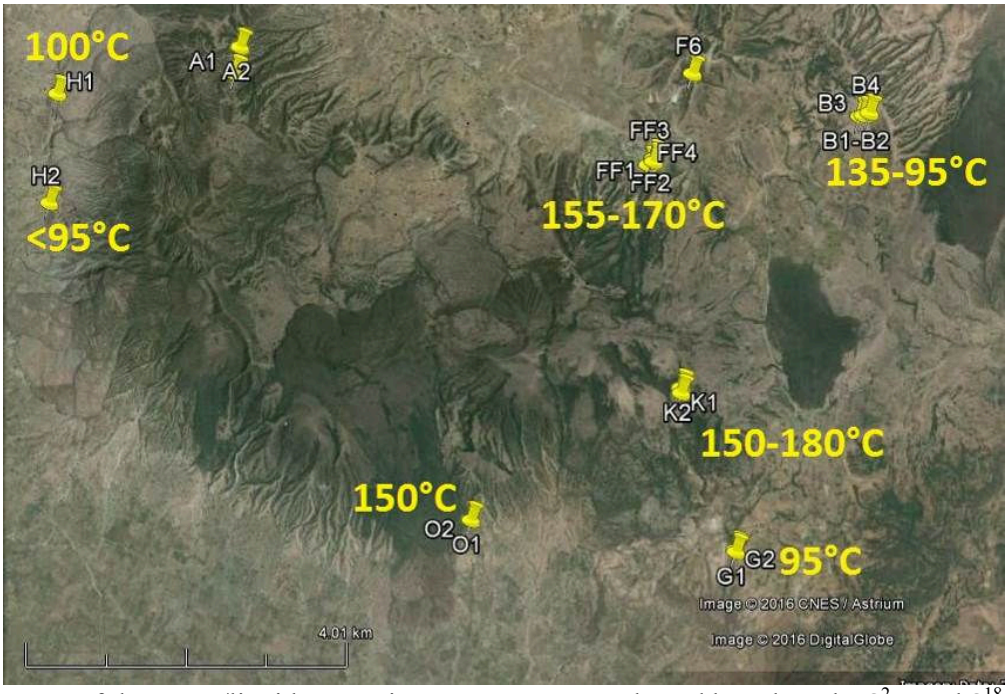

Figure 7: Map of the vapor/liquid separation temperatures evaluated based on the δ^2H and $\delta^{18}O$ values of steam condensates for the Aluto fumaroles and steaming grounds sampled during this work.

A few words of caution are needed concerning the exact values of the vapor/liquid separation temperatures, in that several assumptions are involved in the calculation of the theoretical effects of boiling and condensation processes on isotope compositions. In particular, it must be noted that:
(1) the reservoir liquids met by the deep wells show significant variations of the δ^2H and $\delta^{18}O$ values and
(2) cooling paths of reservoir liquids through conductive heat loss and mixing (before boiling) might lead to isotope values and initial boiling temperatures different from those considered above and consequently to distinct "lines of vapors".
Nevertheless, looking at Figure 6 from a qualitative point of view, there is no doubt that the condensation lines of Kure, Oitu, Finkilo and sample B1 from Bobessa are above the condensation lines of Gebiba, Auto, Hulo, and samples B3 and B4 from Bobessa, leading to higher vapor/liquid separation temperatures for the fumarolic manifestations of the first group.

6. THE $\delta^{13}C$ VALUE OF CARBON DIOXIDE

As shown by the plot of the $\delta^{13}C$-CO_2 value vs. the fraction of ASW in the gas mixtures (Figure 8a), the practically ASW-free fumarolic gases of Finkilo and Gebiba have relatively high $\delta^{13}C$-CO_2 values, varying from -3 to -3.9 ‰, whereas the other gas mixtures, containing significant proportions of ASW, exhibit highly different $\delta^{13}C$-CO_2 values, spanning the range -3.2 to -5.7 ‰.

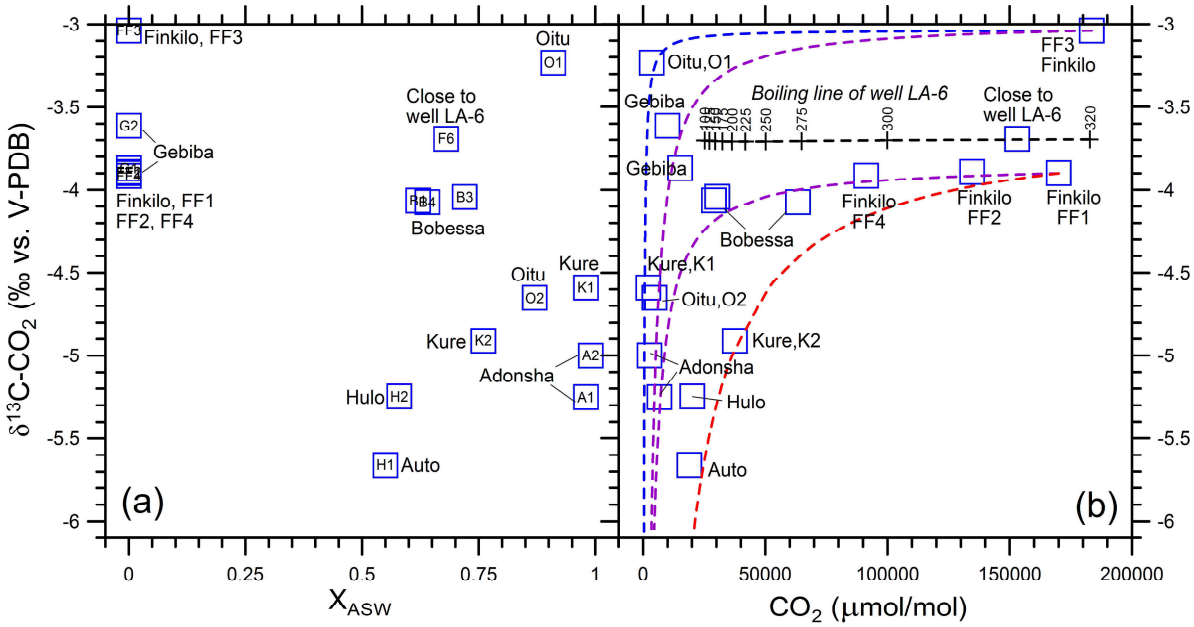

Figure 8: Plots of (a) $\delta^{13}C$-CO_2 vs. the fraction of ASW and (b) $\delta^{13}C$-CO_2 vs. CO_2 content on a total fluid basis for the gas samples collected from the Aluto fumarolic manifestations during this work. The mixing lines between deep gases and organic-CO_2 endmember of red, violet and blue color refer to CO_2 concentrations of 2500, 500, and 50 μmol/mol, respectively, in the organic-CO_2 endmember. The black dashed line with crosses refers to single-step steam separation from the single-phase reservoir liquid of well LA-6 (sample collected in 2000). See text for further details.

The relatively high $\delta^{13}C$-CO_2 values of Finkilo and Gebiba fumarolic fluids either compare with or are somewhat higher than those of the reservoir liquids encountered by wells LA-3, -4.7 ‰, and LA-6, -3.9‰, and other deep gases from the East African Rift System, suggesting that also the CO_2 of Finkilo and Gebiba fumarolic fluids is entirely of deep origin, that is magmatic and/or mantellic.
Considering the abundant amounts of ASW in all the other fumarolic fluids, it seems likely that their CO_2 is partly of deep origin and partly of shallow origin. The shallow CO_2 is typically produced by biologically-mediated processes occurring in soils, such as decay of organic substances and root respiration. The isotopic composition of soil CO_2 has a bimodal distribution with peak values at -17 e -24‰ approximately, reflecting the presence of plants using either the C_4 pathway of carbon fixation (or Hatch-Slack or Kranz) or the C_3 pathway (or Calvin-Benson or non-Kranz), respectively (e.g., Deines, 1980).
The problem is to understand why some ASW-rich fumarolic fluids (i.e., sample O1 from Oitu, sample F6 from the steaming ground close to well LA-6, and samples B1, B3, and B4 from Bobessa) have high $\delta^{13}C$-CO_2 values. To gain insights into this matter let us consider the plot of $\delta^{13}C$-CO_2 vs. CO_2 concentration on a total fluid basis (Figure 8b) in which the spread of points is consistent with a hyperbolic relation between the two considered variables. This hyperbolic relation is explained by mixing between: (i) deep CO_2-rich gases with $\delta^{13}C$-CO_2 values varying from -3 to -3.9 ‰ and (ii) shallow CO_2-poor gases with the typical $\delta^{13}C$-CO_2 values of organic-derived CO_2. The following binary mixing equation (Faure, 1986) describes the mixing process of interest:

$$\delta^{13}C_M = \frac{\delta^{13}C_D \cdot C_{CO_2,D} \cdot x + \delta^{13}C_S \cdot C_{CO_2,S} \cdot (1-x)}{C_{CO_2,M}} \quad (1)$$

where subscripts M, D, and S identify the binary mixture, the deep CO_2-rich gases and the shallow CO_2-poor gases and x is the fraction of the deep gases in the mixture. Note that the binary mixing lines described by this equation are hyperbolae in the $\delta^{13}C$-C_{CO_2} space, if $C_{CO_2,D} \neq C_{CO_2,S} \neq C_{CO_2,M}$, whereas they are straight line if $C_{CO_2,D} = C_{CO_2,S} = C_{CO_2,M}$. The second condition is generally very unlikely and, in fact, it does not apply to the case of interest. Equation (1) has been used to obtain the mixing lines drawn in Figure 8b assuming for the shallow gases a $\delta^{13}C$-CO_2 value of -28 ‰ and different CO_2 concentrations, namely:
- 50 and 500 μmol/mol for the blue and violet mixing lines, respectively, also involving a deep CO_2 gas with the chemical and isotopic characteristics of sample FF3 of Finkilo;
- 500 and 2500 μmol/mol for the violet and red mixing lines, respectively, also involving a deep CO_2 gas with the chemical and isotopic characteristics of sample FF1 of Finkilo.
In this way it is possible to explain the $\delta^{13}C$-CO_2 values and CO_2 concentrations of all the gas mixtures containing significant proportions of ASW. In particular, the high $\delta^{13}C$-CO_2 value of sample O1 of Oitu indicates mixing between a deep CO_2 similar to the Finkilo sample FF3 and a shallow gas with a very low CO_2 concentration. The nearby sample O2 appears to be produced instead by mixing between a deep CO_2 similar to the Finkilo sample FF1 and a shallow gas with a significant CO_2 concentration. Hence, it is necessary to assume important variations in the CO_2 concentrations of the gases originated in soils.
The boiling line is drawn to explain the different CO_2 concentrations and the similar $\delta^{13}C$-CO_2 values of Finkilo and Gebiba fumaroles, which are the only two manifestations where gases rich in CO_2 and practically ASW-free are discharged. The boiling line refers to single-step steam separation from the single-phase reservoir liquid of well LA-6 (sample collected in 2000). This process causes a decrease of 0.74 ‰ units in the $\delta^{13}C$ value of aqueous CO_2, from the arbitrarily assumed initial value of -3.72 ‰ at 320°C to the final value of -4.46 ‰ at 100°C. However, the $\delta^{13}C$ value of gaseous CO_2 remains practically constant at -3.70 to -3.71 ‰ owing to the variation of the $CO_{2(aq)}$-$CO_{2(g)}$ fractionation factor with temperature.

7. CONCLUSIONS

The highest vapor/liquid separation temperatures derived from the δ^2H and $\delta^{18}O$ values of steam condensates are found: (a) along the NNE-trending Jawe Fault, passing through Finkilo and possibly Oitu, and (b) along the NNE-trending tectonic structure passing through Kure and possibly Bobessa (Figure 7). Consequently, these tectonic structures locally act as main upflow zones of the Aluto-Langano geothermal system. In contrast, the peripheral fumarolic manifestations of Gebiba, Auto and Hulo have low vapor/liquid separation temperatures based on the δ^2H and $\delta^{18}O$ values of steam condensates, indicating that they may represent lateral discharge zones of the Aluto geothermal system. These findings agree with those provided by gas geothermometers for Gebiba and solve the ambiguity on the gas separation temperatures given by gas geothermometers at Finkilo.
The $\delta^{13}C$ values of CO_2 suggest a deep origin for the fumarolic fluids of Finkilo and Gebiba. This deep CO_2 mixes with shallow CO_2 produced by biologically-mediated processes occurring in soils in all the other fumarolic sites. The indications provided by the chemical and isotopic characteristics of Aluto fumarolic fluids helped to refurbish the conceptual model of the Aluto-Langano geothermal system.

REFERENCES

Arnórsson, S.: Gas chemistry of the Krísuvík geothermal field, Iceland, with special reference to evaluation of steam condensation in upflow zones. *Jökull*, 37, (1987), 32-47.

Chiodini, G., Marini, L.: Hydrothermal gas equilibria: The H_2O-H_2-CO_2-CO-CH_4 system. *Geochim. Cosmochim. Acta*, 62, (1998), 2673-2687.

Craig, H., Lupton, J.E.: Isotopic geochemistry and hydrology of geothermal waters in the Ethiopian Rift Valley. Scripps Inst. Oceanogr. Ref. Ser. 77-14, (Techn. Rep. UNDP and the Ethiopian Government) (1977), 140 pp.

Darling, W.G.: Hydrothermal hydrocarbon gases: 2, Application in the East African Rift System. *Appl. Geochem*., 13, (1998), 825-840.

Darling, W.G., Talbot, J.C.: Evaluation and Development of Gas Geothermometry for Geothermal Exploration in the East African Rift System. Report of the British Geological Survey Technical WD/91/72, (1991), 59 pp.

Darling, W.G., Gizaw, B., Arusei, M.K.: Lake-groundwater relationships and fluid-rock interaction in the East African Rift Valley: isotopic evidence. *Journal of African Earth Sciences*, 22, (1996), 423-431.

Deines, P.: The isotopic composition of reduced organic carbon. In: P. Fritz, J.C. Fontes (Eds.) Handbook of Environmental Isotope Geochemistry, The Terrestrial Environment 1A, (1980), 329–406.

Faure, G.: Principles of Isotope Geology, 2nd Ed., Wiley, New York, (1986), 589 pp.

Giggenbach, W.F.: Redox processes governing the chemistry of fumarolic gas discharges from White Island, New Zealand. *Appl. Geochem*., 2, (1987), 143-161

Giggenbach, W.F.: Chemical techniques in geothermal exploration. In *Application of Geochemistry in Geothermal Reservoir Development*. (F. D'Amore, co-ordinator), UNITAR, (1991), 119-144.

Giggenbach, W.F.: Relative importance of thermodynamic and kinetic processes in governing the chemical and isotopic composition of carbon gases in high-heatflow sedimentary basins. *Geochim. Cosmochim. Acta*, 61, (1997), 3763-3785.

Giggenbach, W.F., Matsuo, S.: Evaluation of results from second and third IAVCEI field workshop on volcanic gases, Mt Usu, Japan, and White Island, New Zealand. *Appl. Geochem*., 6, (1991), 125-141.

Giggenbach, W.F., Stewart, M.K.: Processes controlling the isotopic composition of steam and water discharges from steam vents and steam-heated pools in geothermal areas. *Geothermics*, 11, (1982), 71-80.

Glover, R.B.: Geochemical investigation in the Lakes District and Afar of Ethiopia. Chemistry Division, D.S.I.R., Wairakei, New Zealand, (1976), 3-35.

Horita, J., Wesolowski, D.J.: Liquid-vapor fractionation of oxygen and hydrogen isotopes of water from the freezing to the critical temperature. Geochim. Cosmochim. Acta, 58, (1994), 3425-3437.

Teklemariam, M., Beyene, K.: Geochemical monitoring of the Aluto-Langano geothermal field, Ethiopia (1999-2001). Geological Survey of Ethiopia, Internal Report, (2002), 44 pp.